

Research of Insertion Mechanism of Flexible Search and Rescue Robot

Linyong Shen, Qian Zhu, Ya Qiu, Yuanfei Cao & Hang Ding
College of Mechatronic Engineering and Automation, Shanghai University, Shanghai, China

ABSTRACT: Due to various factors, the global scope disaster events occur inevitably every year. Terrorism, natural disasters or destructive earthquakes tend to cause a large number of people buried in the ruins of buildings. The research of search and rescue instruments research is mainly focused on snake-like robot and life detector both at home and abroad. The endoscopic search and rescue robot in this paper combines the characteristics of these two kinds of search and rescue equipment. This thesis mainly studies the insertion mechanism of endoscopic flexible search and rescue robot. Based on the mechanics characteristics of the flexible robot body, this paper analyzes several common failure modes during the insertion into the ruins. This article puts forward the scheme of segmented gradual pulling-pushing, which plays an important role in promoting search and rescue work.

Keywords: robot; search and rescue; insertion mechanism

1 INTRODUCTION

Due to various factors, the global disaster events occur inevitably every year. Terrorism, natural disasters or destructive earthquakes tend to cause a large number of people buried in the ruins of buildings. Using scientific methods and advanced technical equipment to rescue the buried people and make the loss to a minimum becomes a hot topic of current research on search and rescue equipment^[1,2]. There are already many research findings about gap search and rescue occurred at home and abroad. Snake-like robot and handheld life detector are both representatives. ACM-R3 invented by Japanese professor Hirose is one of the typical snake-like robots, which is driven by a series of modular joints in a flexible way^[3]. H S1-S5 is currently the world's leading snake-like robot, and the RoboSnake designed by National University of Defense Technology is the earliest reported snake-like robot at home. Handheld life detector, represented by American "Snake Eyes" RTK616 and ZISTOS "Hawkeye", has a small size and is convenient to carry^[4]. Handheld life detector can intuitively find the trapped person by using the optical probe and cables into the ruins. The CCD sensors in handheld life detector would send the video messages to the display terminal. The snake-like robot is too complicated and it is hard to get into the gaps and narrow spaces. Handheld life detectors, such as "Snake Eyes", still on the stage of manual sending which makes the operating personnel in a risk during the process of search and rescue.

This paper provides an automatic insertion way based on endoscopic gap search and rescue robot. The method uses the segmented gradual pulling-pushing method to send the endoscope. This paper analyzes the automatic insertion mechanism of endoscope at first. Based on the flexible structure characteristic, the pa-

per analyzed the mechanics characteristics of the flexible endoscope. Insertion failure may happen due to the mechanical properties of flexible endoscope in the process of sending. For this kind of situation, this paper also analyzes some kinds of failure situations, and summarized the mechanical properties of insertion process, proposed segmented gradual pulling-pushing method. All of these give a theoretical basis for the insertion mechanism of endoscope.

2 ANALYSIS OF AUTOMATIC GRADUAL PULLING-PUSHING INSERTION MECHANISM

2.1 Structure characteristics of endoscope

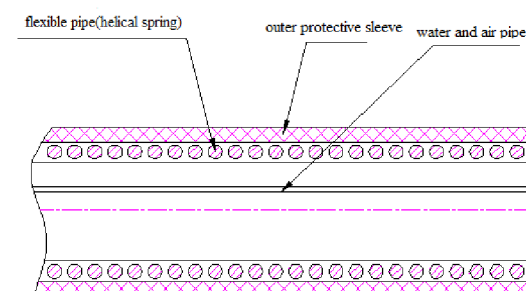


Figure 1. Structure of endoscope

Robot is consisted of flexible endoscope. With a flexible body, the outer ring of endoscope is made up by helical spring. In the endoscope, there are two pipes to provide water and air separately. Outside the endoscope it is an outer protective sleeve made up by the wire mesh material, coated with polyurethane to re-

duce the friction. Structure of endoscope is shown in Figure 1. The coil spring structure makes the body have a good softness in the axial direction, with large stiffness in the radial direction. This structure features make it possible to send the endoscope by pulling-pushing method.

2.2 Compressive mechanical properties

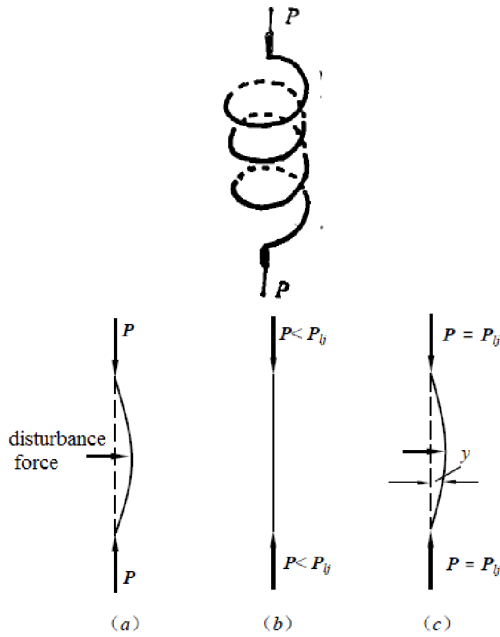


Figure 2. Load and deformation of endoscope

Because of the structure characteristics, the endoscope can be sent into the gap of ruins by insertion mechanism. But considering the mechanics characteristics of helical spring structure, the body may suffer compression bending when the axial propulsive force reaches a certain level.

As shown in Figure 2, assuming that pressure and the axis are coincident. When pressure gradually increases, and no more than a certain limit, the endoscope would keep the shape of straight line. Even though a tiny lateral disturbance force is used to make the body slightly bend, it can still restore line shape after disturbance force is removed. But when pressure increases to a certain limit, the balance becomes unstable, and will not restore after the force is removed. Instead, the body would keep in a curve shape balance. This pressure limit is called critical load, denoted as P_{ij} .

If there is no bending, the propulsion can be along the endoscope, and overcome frictional resistance to send the endoscope. If bending happens, the propulsion can only increase the bending. This compression bending phenomenon happens because the spring suffers compressed load, as shown in Figure 2. When pressure value exceeds the critical load, instability

phenomenon appears in spiral spring, and the spring causes buckling.

As shown in Figure 2, circle angle of n-turn spring is φ . The radius is R with circular cross section of the spring. A pair of pressure P is applied across the center line in opposite direction. The critical load can be calculated by balance equation [5]:

$$P_{ij} = \frac{EJ}{2\nu R^2} \left(\sqrt{\sin^2 \varphi + \frac{1}{n^2} + \frac{4}{n}} - \sin \varphi \right) \quad (1)$$

In the formula, ν is Poisson's ratio and EJ is bending strength. By the above formula, the greater the screw pitch is, the larger $\sin \varphi$, and the smaller the critical load, the more number of turns, and the smaller the critical load is.



Figure 3. Compression model of the endoscope

As shown in Figure 3, in the process of insertion, P is the front resistance, F_{send} is the main propulsion, and $F_{send} \geq P$. To ensure that the flexible endoscope will not bend, then:

$$P < P_{ij} \quad (2)$$

So:

$$F_{send} < P_{ij} = \frac{EJ}{2\nu R^2} \left(\sqrt{\sin^2 \varphi + \frac{1}{n^2} + \frac{4}{n}} - \sin \varphi \right) \quad (3)$$

By the above formula, the greater the screw pitch is, the larger $\sin \varphi$, and the smaller the critical load, the more number of turns, and the smaller the critical load is. The critical load need to be as large as possible, so dense coil spring is chose to make the spring angle as small as possible. In order to avoid too many turns of spring, compression length should not be too long to exceed the critical length.

$$l_{cr} = 2\pi R n t g \varphi \quad (4)$$

Putting it into formula (3), we can obtain:

$$P_{ij} = \frac{EJ}{2\nu R^2} \left(\sqrt{\sin^2 \varphi + \frac{(2\pi R t g \varphi)^2 + 8l_{cr} \pi R t g \varphi}{l_{cr}^2}} - \sin \varphi \right) \quad (5)$$

In the above formula, EJ is associated with the bar section of dense coil spring. Spring coil angle φ is determined by dense coil spring. Therefore the critical load only relate to the compression critical length of endoscope.

In actual situation, the radius of spring tube is 5.5 mm. The screw pitch is $h = 4mm$. Spring coil angle φ is calculated in the trigonometric function:

$$\sin \varphi = 0.0578, \quad \operatorname{tg} \varphi = 0.058,$$

$$\operatorname{tg} \varphi = \frac{h}{2\pi R} = \frac{0.004}{2 \times 3.14 \times 0.0055} = 0.1158 \quad (6)$$

$$\sin \varphi = \frac{h}{\sqrt{(2\pi R)^2 + h^2}} = 0.115 \quad (7)$$

Relationship between number of turns of dense coil spring and the endoscope compression critical length is shown as follows:

$$n = \frac{l_{cr}}{2\pi R \operatorname{tg} \varphi} = \frac{l_{cr}}{h} = \frac{l_{cr}}{2 \times 10^{-3}}$$

(8)

Putting Formula (8) into formula (3), we can obtain :

$$P_{ij} = \frac{EJ}{2\nu R^2} \left(\sqrt{\sin^2 \varphi + \frac{4 \times 10^{-6}}{l_{cr}^2} + \frac{8 \times 10^{-3}}{l_{cr}}} - \sin \varphi \right) \quad (9)$$

Poisson's ratio of spring steel $\nu = 0.26 \sim 0.32$ (0.30). Tensile modulus of elasticity of spring steel $E = 200900 - 203950$ MPa(202000MPa). Spring section is 2 mm diameter circle. Moment of inertia of spring is as follows:

$$J = \frac{\pi d^4}{64} = \frac{3.14 \times 0.002^4}{64} = 7.85 \times 10^{-13} m^4 \quad (10)$$

Putting formula(10) into formula (9), we obtain the relationship between critical load of endoscope and compression critical length as the diagram below:

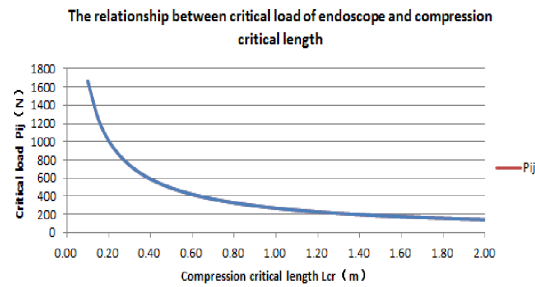


Figure 4. Relationship between critical load of endoscope and compression critical length

Actually, due to the installation limitation, we assume that compression length of endoscope is $l_{cr} = 0.5m$, and put it into formula (9), and calculate critical load: $P_{ij} = 489N$

2.3 Mechanical properties of pushing bend

In the above assumptions of calculation, the force the endoscope bears is completely straight, and only along the axis. So the critical load calculated is very big. In actual cases, the endoscope has bending, bearing not only axial force and bending moment exists. Therefore, the endoscope moment load will be discussed in following paragraph.

Considering the couple M_0 applied on both ends of the spring, spring bends by pressure. There are internal forces on the spring rod whose central angle is α , such as bending moments M_{a1} , M_{a2} and torque T_a . Each two of the three forces are vertical [6], as shown in Figure 5.

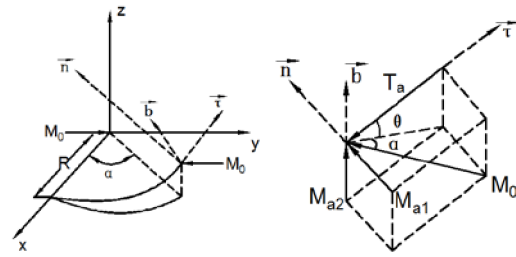


Figure 5. Analysis of internal forces on the spring rod

From Figure 5, we can see:

$$\begin{aligned} M_{a1} &= M_0 \sin \alpha \\ M_{a2} &= M_0 \cos \alpha \sin \theta \\ T_a &= M_0 \cos \alpha \cos \theta \end{aligned} \quad (11)$$

Then calculate strain energy of each circle:

$$U = \frac{1}{2EI} \int_0^{2\pi R / \cos \theta} (M_{a1}^2 + M_{a2}^2) ds + \frac{1}{2GI_p} \int_0^{2\pi R / \cos \theta} T_a^2 ds \quad (12)$$

For the spring rod with circular cross section,

$$\begin{aligned} I_P &= I, G = \frac{E}{2(1 + \mu)}, \text{ and then,} \\ U &= \frac{\pi R M_0^2}{2EI} \cdot \frac{2 + \mu \cos^2 \theta}{\cos \theta} \end{aligned} \quad (13)$$

The deformation energy of the spring is:

$$U = \frac{\pi n R M_0^2}{2EI} \cdot \frac{2 + \mu \cos^2 \theta}{\cos \theta} \quad (14)$$

Bending Angle is:

$$\theta = \frac{dU}{dM_0} = \frac{2\pi R M_0}{2EI} \cdot \frac{2 + \mu \cos^2 \theta}{\cos \theta} \quad (15)$$

According to the calculation of bending beam, $(EI)_{eq}$ is used here as a bending rigidity^[7].

$$\frac{M_0}{(EI)_{eq}} = \frac{1}{\rho}, \rho\theta = l_{cr} = 2\pi Rntg\varphi \quad (16)$$

So:

$$(EI)_{eq} = M_0 \frac{L}{\theta} = \frac{M_0 2\pi Rntg\varphi}{\frac{\pi nRM_0 (2 + \mu \cos^2 \varphi)}{EI \cos \varphi}} = \frac{2EI \sin \varphi}{2 + \mu \cos^2 \varphi} \quad (17)$$

A bending rigidity only has relationship to spring itself, so: $(EI)_{eq} = 0.0318$.

So it can be calculated according to Euler's formula:

$$P = \frac{\pi^2 (EI)_{eq}}{0.5l_{cr}^2} \quad (18)$$

The relationship between bending critical load and compression critical length is shown below:

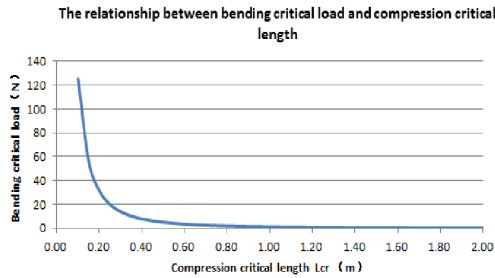


Figure 6. Relationship between bending critical load and compression critical length

From the figure above, the bending critical load is much smaller than the number only bearing the axial force. It is closer to actual number. Assuming that the compression length of the endoscope $l_{cr} = 0.5m$, the critical load $P_{ij} = 5N$.

3 FAILURE ANALYSIS OF SEGMENTED GRADUAL PULLING-PUSHING METHOD

As the mechanical properties mentioned in previous section, there exist the following two kinds of failure modes if we merely push or pull the endoscope of the search and rescue robot into the narrow gap.

3.1 Pushing failure

If merely push the endoscope, due to the Euler critical load mentioned in the previous section (as shown in Figure 7), when the compression length of the flexible endoscope is more than the compression critical length, or the propulsive force applied at the back-end of the

endoscope is greater than the critical force, the bending instability will occur and the propulsion will fail partly or even all.

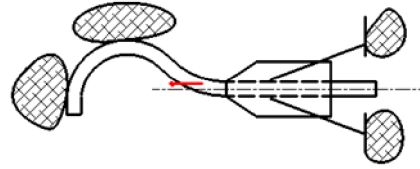


Figure 7. Bending instability of endoscope

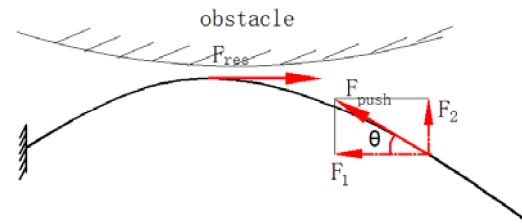


Figure 8. Mechanical model of bending instability

In Figure 7, due to bending instability, compression buckling deformation of the endoscope happens. The actual situation can be simplified to mechanical model shown in Figure 8.

Because $F_{push} > F_{ij}$, the endoscope bends by pressure. Because propulsive force is always along the direction of the endoscope, bend of the endoscope results in deviation from the specified direction. The diagram assumes that the deviation Angle is θ . Then F_{push} can be resolved into F_1 and F_2 , and the relationships of F_1 , F_2 , F_{res} , F_{push} are as follows:

$$\begin{aligned} F_1 &= F_{push} \cos \theta \\ F_2 &= F_{push} \sin \theta \\ F_{res} &= f \cdot F_2 \end{aligned} \quad (19)$$

When $F_1 > F_{res}$, endoscope can be sent into gap smoothly. Based on the above formula, F_1 decreases with the increase of θ , while F_2 increases with the increase of θ . F_1 in the opposite direction of resistance can make the endoscope overcome resistance to move forward. However, F_2 causes the bending situation to become more and more serious, leading to the increase of deviation angle. The increase of θ will cause F_2 to increase and cause F_1 to decrease. Simultaneously, the effect of F_2 causes the pressure between the endoscope and the barrier surface of ruins to increase. Because F_{res} have relations to surface materials of the endoscope and the pressure of the endoscope to the surface of ruins, the increase of pressure of endoscope surface causes F_{res} to increase. Therefore, the continuous decrease of F_1 and the continuous increase of F_{res} will make it unable to overcome the resistance.

3.2 Pulling failure

If merely pull the endoscope at the front-end, the friction will increase with the increase of pulling length and the obstacles of ruins make the endoscope to bend. As shown in figure 9, due to the pulling distance is too long, the back of the endoscope bend. Pulling force will be difficult to overcome the friction. At this time the pulling force will fail, as mechanical model shown in Figure 10.

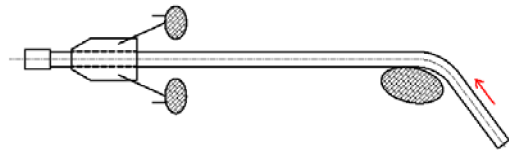


Figure 9. Pulling failure of endoscope

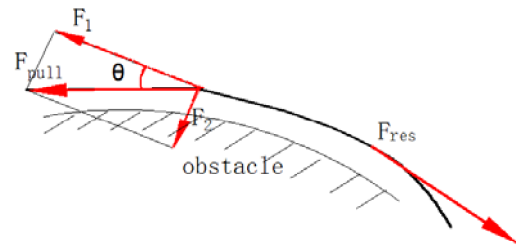


Figure 10. Mechanical model of pulling failure

Due to the increase of pulling distance, the endoscope bends in the gap of ruins. The pulling force of the front-end pulling mechanism cannot be fully used to overcome the frictional resistance. The diagram assumes that the deviation Angle is θ . Then F_{pull} can be resolved into F_1 and F_2 , and the relationships of $F_1, F_2, F_{res}, F_{pull}$ are as follows:

$$\begin{aligned}
 F_1 &= F_{pull} \cos \theta \\
 F_2 &= F_{pull} \sin \theta \\
 F_{res} &= f \cdot F_2
 \end{aligned}
 \tag{20}$$

When $F_1 > F_{res}$, endoscope can be sent into gap smoothly. Based on the above formula, F_1 decreases with the increase of θ , while F_2 increases with the increase of θ . F_1 in the opposite direction of resistance can make the endoscope to overcome resistance to move forward. However, F_1 causes the pressure of the endoscope to the surface to become bigger. Because F_{res} have relations to surface materials of the endoscope and the pressure of the endoscope to the surface of ruins, the increase of pressure of endoscope surface cause F_{res} to increase. Therefore, when the bending angle θ is big enough, F_1 will not be able to overcome F_{res} , the endoscope will not be able to be sent into gap.

Due to the motor torque limitation, we assume that

propulsion $F_{push} = 5N$ or pulling force $F_{pull} = 5N$. According to reference, the coefficient of friction between the endoscope and rock is $0.6 \sim 1.5$, so we use the smallest value to calculate $f \geq 0.6$. The relationship among F_1 , resistance and the deflection angle θ is shown in the figure below:

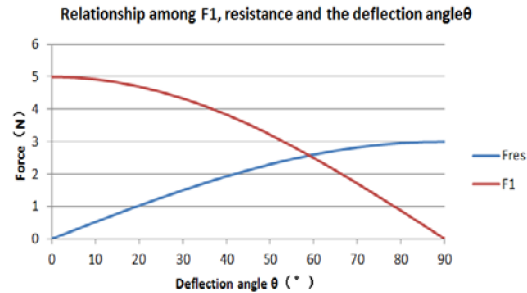


Figure 11. Relationship among F_1 , resistance and the deflection angle θ

When bending deflection angle θ is greater than 58° , F_1 which is along the direction to overcome resistance cannot overcome resistance, leading to pushing failure. When in the state of instability, propulsion will make the endoscope bend further.

During the process of pulling, if pulling distance is too long and the bending of the endoscope caused by the environment of ruins is more than 58° , the pulling force will not be able to overcome the friction, and there will be a pulling failure.

3.3 Segmented gradual pulling-pushing automatically insertion method

As the mechanical properties mentioned in previous section, there exist the following two kinds of failure modes if we merely push or pull the endoscope of the search and rescue robot into the narrow gap.

By above knowable, there will be pushing failure or pulling failure if we merely push or pull the endoscope of the search and rescue robot into the narrow gap. So this paper has proposed a segmented gradual pulling-pushing automatically insertion method, which can effectively avoid the bad phenomena mentioned above.

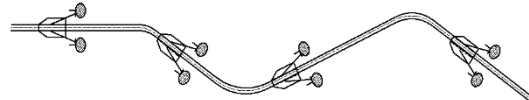


Figure 12. Installation of pulling-pushing mechanism

During actual insertion period, multistage pulling-pushing mechanisms are installed on the endoscope. Any two mechanisms can constitute a set of relative motion institutions, which form a combination

of pushing and pulling, known as “pulling-pushing mechanism”. Therefore endoscope can be gradually sent into narrow gap, as shown in Figure 12.

Two arbitrary adjacent pulling-pushing mechanisms’ installation distance should not be greater than the compression critical length of the endoscope, so that the pushing failure will not happen. Simultaneously, the combination of multistage relative motion mechanism and pulling-pushing also can effectively avoid too long pulling distance and pulling failure.

4 DESIGN OF EXPERIMENTAL PLATFORM AND EXPERIMENTAL VERIFICATION

4.1 Automatically insertion mechanism structure and design of experimental environment

At the final period of design, prototype experiments are carried out. The automatically insertion mechanism structure is shown in Figure 13. The real object is shown in Figure 14. The insertion mechanism is composed of two symmetrical parts, installed outside the endoscope, preloaded by applying pre-tightening force.

The implementation of the segmented gradual pulling-pushing automatically insertion mechanism is friction wheel gradual pushing. Friction wheel transmission diagram is shown in Figure 15. The expanding of stretch stents and tailgates are controlled by the planetary gear train.

Motors drive the friction wheel rotation through the bevel gear transmission, which can push the flexible endoscope to move forward. Simultaneously, the sun wheel of planetary gear train is sheathed on the friction wheel shaft. The motor drives the sun wheel and the sun wheel drives the planet wheel rotation, until the planet wheel rotate to limit position. Then the sun wheel idling and the stretch stents of the insertion mechanism have expanded to the limit position.

The experimental environment is simulation environment of ruins built by bricks. The experiment mainly simulates the turning and climbing situation in ruins.

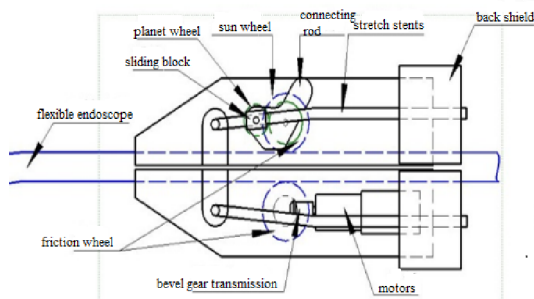


Figure 13. Automatically insertion mechanism structure



Figure 14. Real object of insertion mechanism

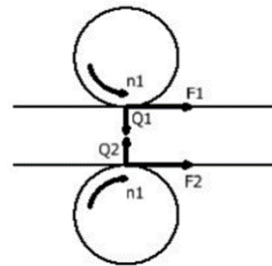


Figure 15. Friction wheel transmission

4.2 The experiment and the analysis of the results

4.2.1 Mechanical property testing of endoscope

The length of the endoscope in the experiment is 10m, the outer diameter is 13mm, and the weight is 2.3 KG. Pulling experiments are conducted on concrete surface. The total sliding friction is 15N.

In fact, in order to avoid the occurrence of bending failure, propulsion must be smaller than the bending critical load. Propulsion must be greater than the friction simultaneously, to overcome the resistance.

If endoscope is sent into gap by a single organization, the pressure the endoscope bears has exceeded its bending critical load and the propulsion has failed inevitably, because the endoscope is too long. While the segmented gradual sending method is adopted to send the endoscopic flexible body into narrow gap, frictional resistance is the only force to overcome. In order to ensure that compression length does not exceed the critical compression length, and bending force does not exceed the critical load.

Endoscope can be divided into 15 segments. Friction resistance of each segment is $f = 1N$. Compression length is 670 mm. Critical bending load is $P = 2.9N$. Assuming that propulsive force is F , safety coefficient is $N = 2$, then if F meets the following formula, the endoscope can be sent into narrow gap successfully.

$$nf \leq F \leq P \quad (21)$$

4.2.2 Mechanical property testing of pulling-pushing method

The endoscope is sent into the gap by the segmented gradual pulling-pushing method. The following experiment can test the bending force of different length of the endoscope. In the experiment, one end of endoscope is fixed, the other end of the endoscope is applied a normal force perpendicular to the endoscope. See Figure 16 below.



Figure 16. Bending experiment

The experimental results are shown in table 1.

Table 1. Relation between the compression length of endoscope and the maximum bending stress

Compression length of endoscope (mm)	1000	600	500	400	300
Maximum bending stress (N)	1	3.5	3.5	4.5	7

4.2.3 Pulling-pushing sending experiment

In this paper, experiment was carried out in view of the situations the endoscope of search and rescue robot may encounter in the rubble. The segmented gradual pulling-pushing method was adopted to send the robot, which simulates the turning situation of ruins.



Figure 17. Pulling-Pushing Sending Experiment

After experimental verification, segmented gradual pulling-pushing mechanism basically can send the endoscope into ruins, but when turning angle is less than 90°, the result is unstable and needs further improvement.

5 CONCLUSION

This paper mainly studies the insertion mechanism of the endoscope of search and rescue robot. The endoscope insertion aims to send the endoscope into ruins by segmented gradual pulling-pushing method. This paper analyzes the mechanical property of the endoscope, discusses several common failure modes, and proposes a segmented gradual pulling-pushing method. This method can avoid the failure situation effectively, greatly improving the efficiency and stability of insertion.

After experimental verification, the segmented gradual pulling-pushing mechanism designed based on this article can send the endoscope of search and rescue robot into ruins successfully. Besides, the mechanism has compact structure, low cost, and even can work under the harsh environment in ruins and provides technical support in the disaster scene. It will obviously have its place in the future.

REFERENCES

- [1] Wang Zhongmin. 2007. Research status and development tendency of searching and rescuing robot. *Modern Electronics Technique*, 30(17): 152-155.
- [2] Zhang Tao, Shang Hong, Xu Jianhua, et al. 2012. Application of robot technology in search and rescue in earthquake ruins. *Journal of Natural Disasters*, 21(5): 108-112.
- [3] Lin Bin. 2003. Research of the snake-like robot and its application in disaster rescue. (3): 22-26.
- [4] Tang Tong, Yang Siqian, Cuiyan, et al. 2012. Uncovering secrets of life detection instrument—the most powerful weapon in disaster rescue. *Disaster Reduction in China*, 7: 026.
- [5] Wu Jike, Huang Yonggang. 1987. The stability problem of elastic curved bar. *Acta Mechanica Sinica*, 19(5): 445-454.
- [6] Tan Meilan. 2000. The strength, stiffness, and stability of the thin ring spiral compression spring. *Journal of East China Shipbuilding Institute*, 14(2): 66-69.
- [7] Timoshenko S P. 1972. *Mechanics of Materials*. USA: Van Nostrand Reinhold Company.
- [8] Cai Zixing. 2000. *Robotics*. Beijing: Tsinghua University Press.
- [9] Wu Xiugen, Zheng Bailin, He Pengfei, et al. 2012. The balance equation of helical spring in critical and instability flexion. *Applied Mathematics and Mechanics*, 33(8): 988-996.
- [10] Shugen. 2001. Analysis of creeping locomotion of a snake-like robot. *Advanced Robotics*, 15(2): 205-224.
- [11] Transteth A A, Leine R I, Glocker C, et al. 2008. Snake robot obstacle-aided locomotion: modeling, simulations, and experiments. *Robotics, IEEE Transactions on*, 24(1): 88-104.
- [12] Que Hao, Zhang Baojun, Qian Jinwu. 2004. The control device for obstacle-avoidance of endoscope. *Mechanics*, 10(1): 32-33.
- [13] Qian Jinwu, Li Yi, Shen Linyong. 2001. Research on

- crawling mechanism of robot in soft pipeline. *Machinery & Electronics*, 1(1): 37-38.
- [14] Hopkins J K, Spranklin B W, Gupta S K. 2009. A survey of Snake-inspired robot designs. *Bioinspiration & Biomimetics*, 4(2): 1-19.
- [15] Ma S, Tadokoro N, Li B, et al. 2003. Analysis of creeping locomotion of a snake robot on a slope[C]//Robotics and Automation, 2003. Proceedings. ICRA'03. IEEE International Conference on. IEEE, 2: 2073-2078.
- [16] Chen Wenmiao, Chen Hua. 1984. Deformation analysis of close-wound helix spring. *Mechanics in Engineering*, 6(6): 49-50.
- [17] Chen Weifeng, Peng Jinchuan, Wang Yunji, et al. 2003. Three types of life detector and its application in earthquake relief. *Earthquake Research in Sichuan*, (3): 25-28.